Lasers in Medical Science (2023) 38:11
https://doi.org/10.1007/s10103-022-03695-w

ORIGINAL ARTICLE

Investigating effects of locally applied boric acid on fracture healing with and without low-level laser therapy

Ferda Turgut[1] · **Latif Emrah Yanmaz**[2]

Received: 14 October 2022 / Accepted: 29 November 2022 / Published online: 21 December 2022

Abstract

This study aimed to investigate the effects on fracture healing of locally applied boric acid (BA) with and without low-level laser therapy (LLLT). A unicortical femoral defect was surgically created on the anterolateral surface of proximal femur of each subject. The subjects, totaling 56 Wistar albino rats, were randomly allocated into four groups ($n = 14$ each): control, LLLT ($\lambda = 905$ µm, 10,000 Hz, 25 mW, and peak power 25 W), BA (40 mg/kg), and BA + LLLT groups. On the 30th day, the highest radiological score was recorded for the BA + LLLT group (3.63 [2–4]), followed by the BA (3.38 [2.75–3.75]), control (3 [2–3.25]), and LLLT (2.5 [1.25–3]) groups. On days 15 and 30 post-surgery, malondialdehyde levels were significantly lower among the BA + LLLT group compared to the control group ($p < 0.001$). On day 30, superoxide dismutase, catalase, and alkaline phosphatase levels were highest in the BA + LLLT group compared to the control group ($p < 0.001$). When the histopathological, immunofluorescence, and immunohistochemical findings on the 15th and 30th days were compared with the control group, a statistically significant difference was found for the BA and BA + LLLT groups ($p < 0.05$). This study suggests that locally applied BA with LLLT may accelerate fracture healing.

Keywords Boron · Borax · BMP-2 · Osteoblast · Photobiomodulation · Photobiostimulation

Introduction

Fracture healing is a complex process that takes place over weeks to years, and it is regulated by genetic, biological, and mechanical factors. This process requires the spatially and temporally coordinated interaction of a large number of cells and molecular mediators [1]. The expected healing time depends on many factors, including the mechanical, biological, and clinical factors used to determine fracture assessment scores [2]. Bone grafts are commonly used in multiple comminuted fractures, delayed callus, or the absence of union in order to stimulate bone fusion after arthrodesis [3].

Boric acid (BA) is the most commonly used boron component in the medical field. BA is an important element thought to affect bone metabolism because it interacts with calcium, vitamin D, and magnesium [4]. Dietary boron deficiency significantly decreases osteogenesis, which changes bone healing [5]. BA helps bones' growth and repair [6], significantly affects preosteoblasts' proliferation and osteogenic differentiation [7] and causes a higher rate of osteoblastic activity [8].

Low-level laser therapy (LLLT), also called *photobiology* or *biostimulation*, is a non-invasive light source therapy that produces light of a single wavelength. It does not emit heat, sound, or vibration. LLLT is believed to affect the function of connective tissue cells (fibroblasts), accelerate connective tissue repair, and act as an anti-inflammatory agent [9]. LLLT can improve the bone formation process [10], and it increases callus volume and bone mineral density [11] and accelerates osteocytes' proliferation [11]. LLLT increases osteoblastic activity, vascularization, the organization of collagen fibers, and adenosine triphosphate levels [12]. LLLT's advantages are that it is easily accessible, does not require simultaneous drug administration, is safe for tissue, and can be applied using incisions or surgical implants [13].

It has been emphasized that boron components have positive effects on fracture healing [8, 14, 15]. There are also many research articles showing that the use of graft materials with LLLT accelerates fracture healing [11, 16]. For

✉ Ferda Turgut
ferda.turgut@atauni.edu.tr

[1] Department of Surgery, Faculty of Veterinary Medicine, Ataturk University, Erzurum, Turkey

[2] Department of Surgery, Faculty of Veterinary Medicine, Burdur Mehmet Akif Ersoy University, Burdur, Turkey

this reason, this study aimed to investigate effects of locally applied BA's on fracture healing among Wistar albino rats with and without LLLT. We hypothesized that BA with LLLT would enhance fracture healing.

Materials and methods

Animals

This study was approved by the Ethics Committee for Animal Experimentation (2021/76) at the Faculty of Veterinary Medicine of Atatürk University in Erzurum, Turkey. This research was conducted between April 2022 and June 2022 at the Atatürk University Medical Experimental Application and Research Center in Erzurum. The study's subjects comprised 56 adult, male, Wistar albino rats (aged 12 weeks and weighing 350 ± 50 g). The rats were maintained under a controlled temperature (22 ± 2 °C) and light–dark environment. They had free access to water and a commercially available diet.

Groups

Each rat was randomly assigned to one of four groups, which each comprised 14 animals, after its unicortical femoral defect (UCD) was created. The groups were determined by treatment, as follows: a control group (no treatment after UCD creation surgery), an LLLT group, a BA group, and a BA + LLLT group. Properly packed BA, which was obtained from the Eti Boron Mining Institute, was sterilized in an ethylene oxide sterilizer and then placed in the UCDs of the BA and BA + LLLT group subjects at a dose of 40 mg/kg. The rats in all groups were sacrificed using a lethal dose of the anesthetic substance sodium pentobarbital (800 mg/kg) on days 15 ($n = 28$, seven animals from each group) and 30 ($n = 28$, seven animals from each group) post-surgery and subjected to radiological, histopathological, and biochemical analysis.

Surgery

Butorphanol was administered subcutaneously at a dose of 0.5 mg/kg for each rat just before its operation, and 1 mg/kg of meloxicam was administered subcutaneously just before the skin incision. A UCD was created while the rats were under general anesthesia via the intramuscular administration of 10 mg of xylazine (Xylazin Bio, 2%, 50 mL, Bioveta) and 100 mg of ketamine (Ketasol 10%, 10 mL, Interhas-Richter Pharma, Wels, Austria). The animals were prepared for surgery and positioned in lateral recumbency. After routine preparation of the operation area, the femoral shaft was reached using an anterolateral approach between the biceps femoris and vastus lateralis muscles. A UCD was created with a 2.8 mm drill on the anterolateral surface of the proximal femur. The defect was irrigated with sterile saline, and BA was locally applied to the UCD for rats in two groups (the BA and BA + LLLT groups). For the other two groups, only sterile saline was applied to the UCD. The subject's subcutaneous tissue and muscles were closed using a continuous suture method (2/0 coated vicryl, Ethicon, USA), and the skin was closed using a separated suture method (nylon 2/0). For all groups, 0.2 mL of a broad-spectrum antibiotic (Rifocin® 125 mg amp., Sanofi-Aventis, Turkey) was applied locally to the UCD area to protect against possible contamination.

Laser application

A GaAs (gallium arsenide) laser device (Lasermed 2200, Eme Phsio, Italy) was set to $\lambda = 905$ µm, 10,000 Hz, 25 mW, and peak power 25 W in a continuous mode used for laser therapy. The device was calibrated before conducting experiments. A monodiode laser probe (MLA1/25) was applied to the anterolateral surface of each rat's femur that had undergone UCD surgery in the LLLT and BA + LLLT groups once daily via direct contact with the skin. The laser treatment was calculated according to the formula $(power/beam\ field) \times time = J/cm^2$, and it was transcutaneously applied at a level of 4 J/cm^2 to a single point for 160 s per day for 2 weeks starting on the first day after the operation. The rats were attended during laser application by the same person who had performed their UCD surgery.

Radiological evaluation

On days 15 and 30 post-surgery, the craniocaudal and mediolateral positions of each rat's femur were with a stationary X-ray machine (Mex-100, Oberhausen, Germany). Tomographic images of the femur were scanned with the rats in lateral recumbency using a Toshiba Asteion four-slice Computed Tomographic system (Toshiba, Tokyo, Japan). CT and radiographic images were simultaneously assessed using mRUST scala [17].

Biochemical evaluation

Blood was taken from the rats, transferred to lithium heparin tubes, and centrifuged at 3000 rpm at + 4 °C for 10 min. Their plasma was separated and stored in a deep freezer at − 20 °C until biochemical analysis was performed. Malondialdehyde (MDA) [18], catalase (CAT) [19], superoxide dismutase (SOD) [20], and alkaline phosphatase (ALP) activity were analyzed with a commercially available ELISA kit (Shangai Coon Koon Biotech Co. Ltd, China) using spectrophotometry (Biotechepocha UV–Visible EIA, USA).

Histopathological evaluation

Bone tissue samples from each rat's UCD were fixed in a 10% buffered formalin solution for 48 h. The detected bone tissue was decalcified in a decalcification solution. After undergoing a routine tissue procedure, the tissue was embedded in paraffin blocks, and 4 µm thick sections were taken from each block. Samples were prepared for histopathological examination, stained with hematoxylin–eosin (H&E), and examined with a light microscope (Olympus BX51, Japan). Sections were examined under the light microscope, and lesions were scored between 1 and 4 by evaluating angiogenesis, necrosis, mononuclear cell infiltration, granulation tissue, fibrosis, and osteoblastic activity according to the area covered by × 40 magnification. For the evaluated criteria, according to the area covered, from 1 to 25% of the total area coverage area was score 1, from 26 to 50% of the coverage area was score 2, from 51 to 75% coverage area was score 3, and from 76 to 100% coverage area was score 4 [21].

Immunhistochemical evaluation

Tissue sections were prepared on adhesive (poly-L-lysin) slides, deparaffinized, and dehydrated for immunoperoxidase examination. After being washed with suppressed endogenous peroxidase activity in 3% H_2O_2, the tissues were boiled in an antigen retrieval solution. To prevent nonspecific background staining in the sections, a protein block compatible with all primary and secondary antibodies was added and incubated for five minutes. TNF-α (CAT [catalase] no.: sc-52746; dilution ratio: 1/100 US) for bone tissue was used as the primary antibody. For examination under light microscopy (ZEISS Axio, Germany), a 3 × 3' diaminobenzidine (DAB) chromogen was used. Sections were evaluated in the ZEISS Zen Imaging Software program. The data were expressed as nm.

Immunofluorescence analysis

Tissue sections were prepared on adhesive (poly-L-lysin) slides, deparaffinized, and dehydrated for immunoperoxidase examination. For bone tissue, primary antibody BMP-2 (CAT no.: ab214821; dilution ratio: 1/100 UK) was added and incubated at 37 °C for 1 h. After washing, secondary FITC (CAT no.: ab6717; dilution ratio: 1/500 UK) was added and incubated at 37 °C for 30 min. DAPI (CAT no.: D1306; dilution ratio: 1/200 US) was dropped onto the washed tissues and incubated in the dark for 5 min, and then the glycerin was sealed. Sections were examined under a fluorescent microscope (ZEISS AXIO, Germany) and were evaluated in the ZEISS Zen Imaging Software program. The data were expressed as nm.

Statistical analysis

For immunohistochemical and immunofluorescence examination, to determine the intensity of positive staining from the obtained images, five random areas were selected from each image. The positive-to-total-area ratio (in percentage terms) was calculated via measurements with the ZEISS Zen Imaging Software program. A one-way analysis of variance test was performed after Tukey's test to compare immunoreactive cells and the immunopositive stained areas of positive antibodies with healthy controls. Independent sample t-test was used to determine the difference between the times of the groups (15th and 30th day). The Kruskal-Wallis test was used to determine the difference between the groups over time for data that were not normally distributed, and the Dunn test was used for multiple comparisons. The Mann Whitney U test was used to determine the difference between the times of the groups (day 15 and 30). All data were analyzed using the statistical package for SPSS software, version 22.0 (IBM Software, Inc. Chicago, USA). A p value of < 0.05 was considered significant. Data were presented as mean ± standard deviation (SD), or median (range).

Table 1 Malondialdehyde (MDA), superoxide dismutase (SOD), catalase (CAT), and alkaline phosphatase (ALP) levels on days 15 and 30 post-surgery

	MDA (mmol/L)		SOD (U/mL)		CAT (kU/L)		ALP (U/L)	
Groups	Day 15	Day 30	Day 15	Day 30	Day 15	Day 30	Day 15	Day 30
Control	35.51 ± 1.08aA	19.34 ± 0.63aC	8.96 ± 0.11cDE	8.17 ± 0.84cE	25.49 ± 0.81cF	94.75 ± 1.13cC	107.07 ± 1.54dE	108.33 ± 1.32bDE
LLLT	25.11 ± 0.59bB	18.83 ± 0.74aC	12.27 ± 0.47bC	11.35 ± 0.72cCD	26.31 ± 0.74cF	101.99 ± 1.78cC	112.33 ± 0.61cCD	112.41 ± 0.66bCD
BA	23.66 ± 0.46bB	13.56 ± 0.85bD	12.47 ± 0.69bC	18.39 ± 0.93bB	60.12 ± 2.69bE	127.36 ± 4.75bB	115.93 ± 0.68bC	122.82 ± 1.64aAB
BA + LLLT	17.06 ± 0.63cC	12.01 ± 0.47bD	15.99 ± 0.33aB	21.94 ± 0.95aA	77.01 ± 2.07aD	195.17 ± 7.84aA	120.98 ± 0.37aB	127.32 ± 0.90aA

The difference between the means in the same column with different lowercase letters (a, b, c) is significant (day 15 separately, day 30 separately; $p < 0.001$). The difference between the means in the same column with different uppercase letters (A, B, C, D, E) is significant (a comparison between the 15th and 30th days; $p < 0.001$)

$p < 0.001$

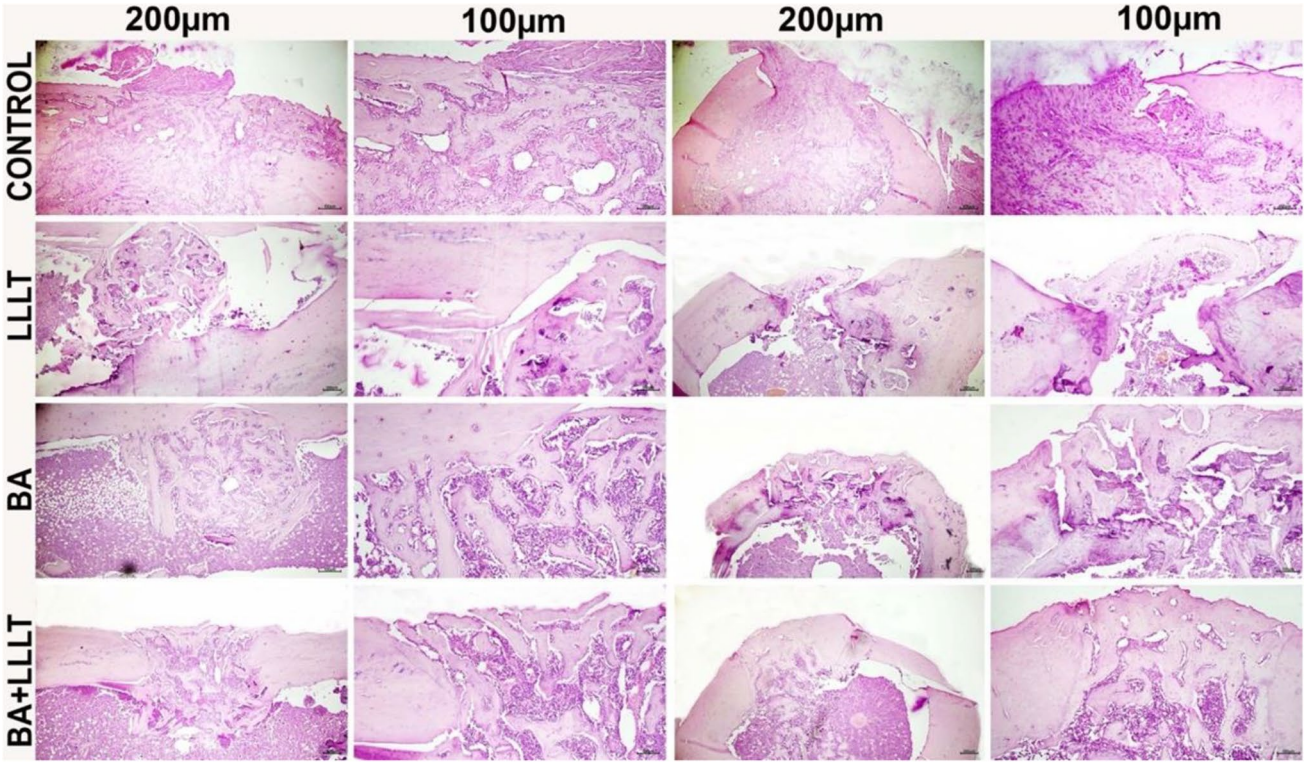

Fig. 1 Histological analysis of transverse and longitudinal sections taken from the unicortical femoral defect (UCD) area of the treatment and control groups on Day 15 post-surgery, H&E, bar: 100–200 µm. Histological analysis of sections from treated and control animals at the unicortical defect site. The drill hole can be seen at 11–1 o'clock in each section. LLLT low-level laser theraphy, BA boric acid

Results

Radiological findings

Bone formation was not observed in the control group's UCD areas on the 15th day post-surgery. On the 15th day, callus formation was observed in the control and BA groups. Also on day 15, bridging was visible in the BA + LLLT group, while each rat's fracture line was still evident. On the 30th day, bridging was observed in the BA + LLLT, BA, and control groups, while no fracture line was observed for rats in the BA + LLLT group, and remodeling had formed. On the 15th day, the best radiological scores were obtained for the BA + LLLT group (3.5 [2.25–4]), followed by the BA (2.5 [2.25–2.75]), LLLT (2.37 [1.5–3]), and control (1.62 [1, 2]) groups. On the 30th day, the best radiological score was obtained for the BA + LLLT group (3.63 [2–4]), followed by the BA (3.38 [2.75–3.75]), control (3 [2–3.25]), and LLLT (2.5 [1.25–3]) groups.

Biochemical findings

On days 15 and 30 post-surgery, MDA levels were significantly lower among the BA + LLLT group compared to the control group ($p < 0.001$). On day 30, SOD, CAT, and ALP levels were highest in the BA + LLLT group compared to the control group ($p < 0.001$) (Table 1).

Histopathological, immunofluorescence, and immunohistochemical findings

When histopathological findings on the 15th day post-surgery were evaluated, fibrous callus had started to form for the control group, versus severe fibrous callus formation for the LLLT group, tight connective tissue formation for the BA group, and severe fibrocartilaginous callus formation in which these fibrous tissues were replaced by chondrocytes. Bone trabeculae were observed to have formed. Inflammation of the bone tissue was severe for the control group, moderate for the LLLT group, and mild for the BA group, but no inflammation was observed for the BA + LLLT group. While osteoblastic activity had just started for the control group, it was observed to be mild for the LLLT group, severe for the BA group, and very severe for the BA + LLLT group.

When osteoblastic activity was examined on the 30th day, it was observed to be mild for the control group, moderate for the LLLT group, severe for the BA group, and very severe for the BA + LLLT group. In addition to osteoblastic activity, severe osteoclastic activity was observed for the BA group, versus very severe for the BA + LLLT group. The UCD was found to have

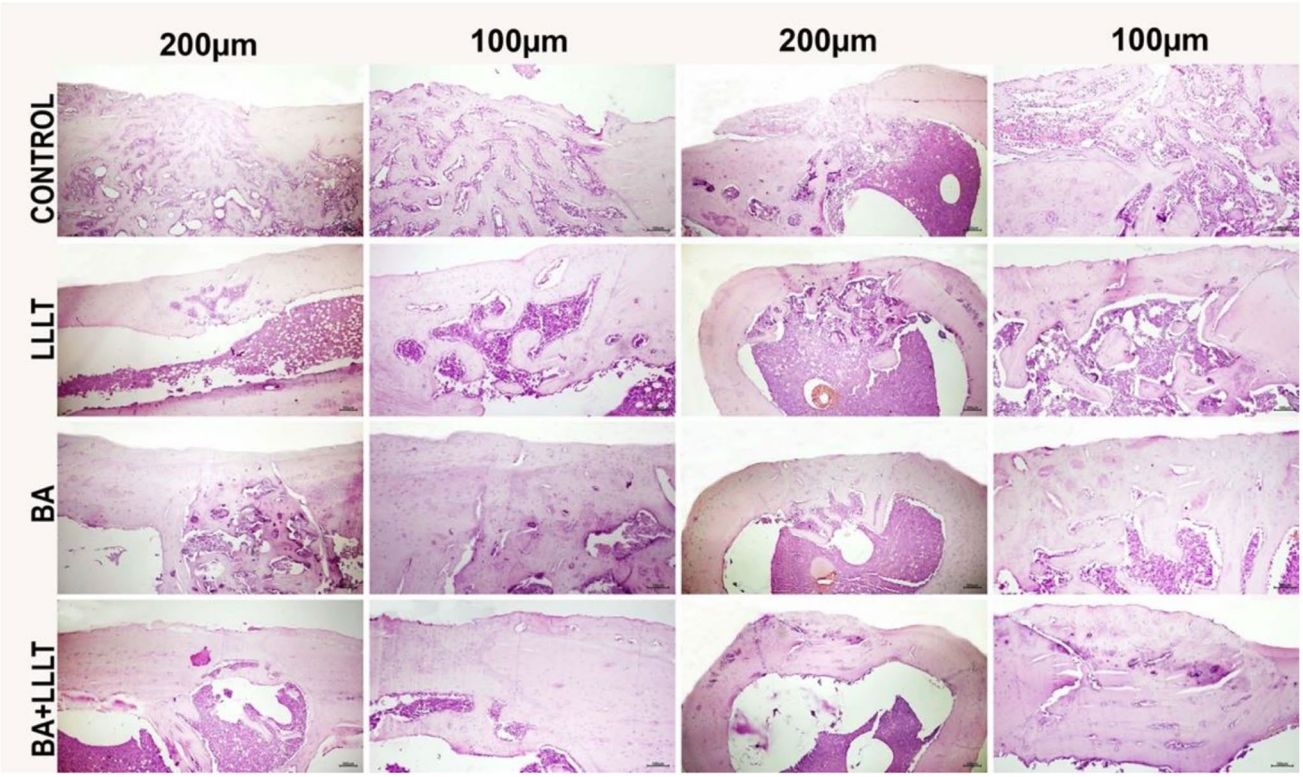

Fig. 2 Histological analysis of transverse and longitudinal sections taken from the UCD area of the treatment and control groups on day 30 post-surgery, H&E, bar: 100–200 µm. Histological analysis of sections from treated and control animals at the unicortical defect site. The drill hole can be seen at 11–1 o'clock in each section

closed for all groups except the control group. For the control group, the UCD was observed to have closed, the chondrocytes had increased, and the fibrous tissue had decreased. The remodeling process was found to have started for the LLLT group. For the BA group, severe bone marrow formation and bone trabeculae formations were observed. Severe bone marrow formation was observed for the BA + LLLT group. When the 15th and 30th days of histopathological findings were evaluated, the control group was scored as grade 1, LLLT group as grade 2, BA group as grade 3, and BA + LLLT group as grade 4 (Figs. 1 and 2).

On the 15th and 30th days, BMP-2 expression in the osteoblasts was mild for the control group, moderate for the LLLT group, severe for the BA group, and very severe for the BA + LLLT group (Fig. 3). On the 15th day, TNF-α expressions in the cytoplasm of the inflammatory cells and around the vessels were mild for the control group, moderate for the LLLT and BA groups, and severe for the BA + LLLT group (Fig. 4). On the 30th day, TNF-α expressions in the cytoplasm of the inflammatory cells and around the vessels were observed to be severe for the control group, moderate for the LLLT and BA groups, and mild for the BA + LLLT group.

The histopathological, immunofluorescence, and immunohistochemical scores for the BA and BA + LLLT groups were significantly higher than those of the control group (Table 2). When the histopathological, immunofluorescence, and immunohistochemical findings on the 15th and 30th days were compared with the control group, a statistically significant difference was found for the BA and BA + LLLT groups ($p < 0.05$).

Discussion

This experimental study aimed to investigate effects of BA on bone formation after co-administration with LLLT as a graft material. Localized BA applied to the bone defects of rats significantly increased bone formation compared to the control group.

Adding BA to mice's drinking water has been shown to increase the presence and activity of osteoblasts and osteoclasts, increasing bone calcium concentration and thereby aiding bone growth and repair [22]. However, a recent study reported that local BA application is more effective than oral administration

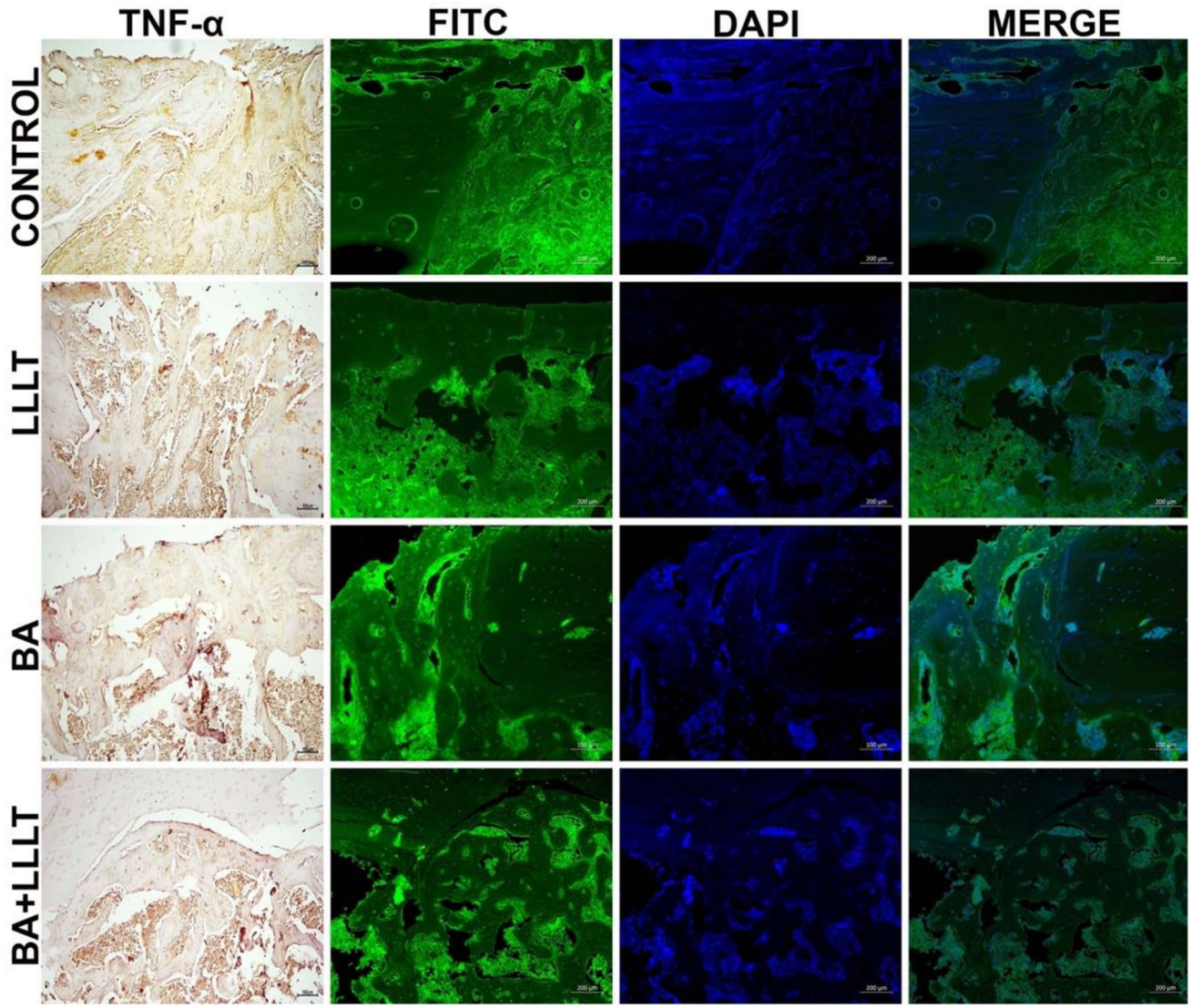

Fig. 3 Immunohistochemical and immunofluorescence analyses of sections taken from the UCD area of the treatment and control groups on day 15 post-surgery, TNF-α expressions, IHC-P, BMP-2 expressions (FITC), IF, bar: 200 µm

[23]. For this reason, we chose to apply BA to the defect, rather than administering BA orally. The local administiration of BA via injection into femoral defects has also been found to cause a higher rate of osteoblastic activity at the early stage of intramembranous bone formation [8]. Similarly, in this study, a local BA application to rat UCD significantly increased the amount and quality of bone formation compared to the control group. Many different BA doses have been used for rats previously [24, 25]. Although the current study did not aim to identify a standard dose of locally applied BA for a fracture model, our observations suggest that 40 mg/kg of BA could be used for rats without any systemic effect. However, more studies are warranted to detect the optimal dose.

LLLT has an anti-inflammatory effect on soft tissues, depending on its wavelength, its dose, and local conditions. LLLT reduces pain and accelerates healing by stimulating cell proliferation [26]. It has been found to increase osteoblastic activity, blood vessels, and the mineralized bone matrix in bone fractures [27]. Additionally, due to LLLT's correlation with calcification, an increase in ALP activity has been observed [28], which is an important marker of bone formation after laser application [29]. Many LLLT factors—such as its wavelength and application time—are still being investigated [30]. Different LLLT doses can be used for cortical defects [11]. The literature includes studies on the use of LLLT for fractures at different wavelengths, strengths, and energy densities by different authors [31–33]. Additionally, various factors—such as cell growth stage, frequency, and number—affect LLLT [33]. An adequate energy display in laser therapy has been much discussed [34, 35], but no dose standardization has been applied to

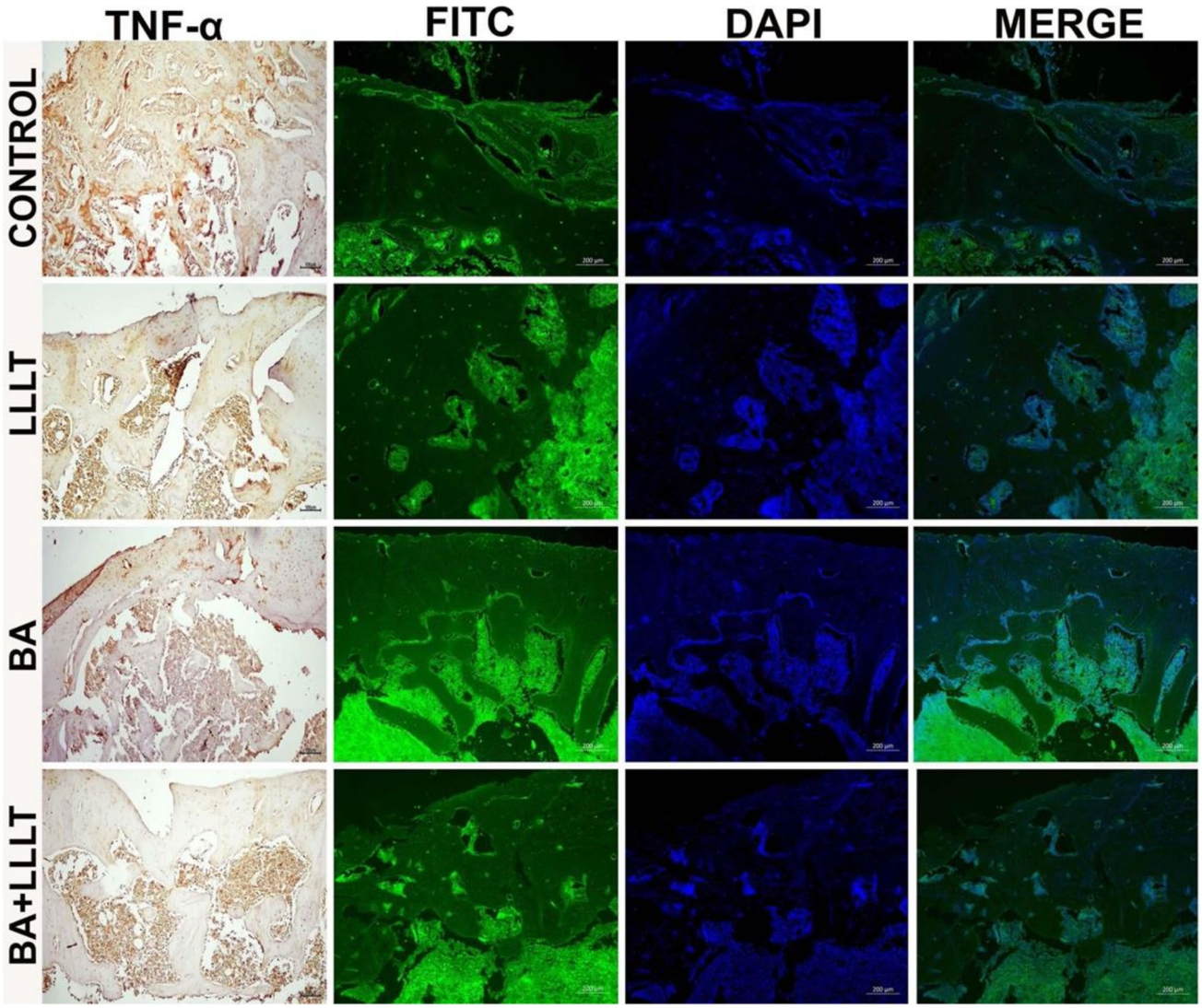

Fig. 4 Immunohistochemical and immunofluorescence analyses of sections taken from the UCD area of the treatment and control groups on day 15 post-surgery, TNF-α expressions, IHC-P, BMP-2 expressions (FITC), IF, bar: 200 µm

achieve ideal photobiomodulation [36]. The parameters used in the current study were continuous irradiation, a wavelength of 905 nm, an energy density of 25 mW, 4.0 J/cm^2, and once-daily therapy of 14 treatments, each lasting 160 s. A similar laser dose has been previously applied to rats' femoral defects [12].

In the current study, radiography and tomography were used to evaluate the mRUST scoring system. It was not clear why in 15

Table 2 Immunohistochemical (TNF-α) and immunofluoresence (BMP-2) results on days 15 and 30 post-surgery

Groups	Day 15		Day 30	
	TNF-α (nm)	BMP-2 (nm)	TNF-α (nm)	BMP-2 (nm)
Control	19.63 ± 1.57^{a}	20.74 ± 4.36^{a}	65.27 ± 3.52^{a}	20.31 ± 4.48^{a}
LLLT	40.11 ± 3.15^{b}	39.31 ± 4.13^{b}	41.43 ± 5.19^{b}	39.18 ± 4.92^{b}
BA	39.52 ± 4.25^{b}	60.14 ± 3.28^{c}	40.98 ± 6.22^{a}	58.91 ± 5.37^{c}
BA + LLLT	60.27 ± 5.21^{c}	79.11 ± 4.34^{d}	25.56 ± 2.35^{c}	79.11 ± 3.61^{d}

Different lowercase letters (a, b, c, d) in the same column represent a statistically significant difference

LLLT low-level laser theraphy, *BA* boric acid

and 30 days the results of the radiological analysis were reversed between the control group and LLLT. This is likely because the mRUST scoring system, which has poor effectiveness for evaluating bony union in the early postoperative period [37].

BA and LLLT treatments decreased MDA levels in unicortical bone defects of rat livers on 15 and 30 days, possibly due to oxidative stress inhibition. After treatment, SOD and CAT activities increased as a result of BA application due to the repression of oxidative stress. Previous studies have demonstrated that oxidative stress occurs during recovery from a fracture, and reactive oxygen species is one factor that negatively affects fracture healing [38, 39]. Increased radical production has been reported to impair fracture healing in examinations performed 22 days after a fracture [40]. Therefore, early periods are extremely important to fracture healing [40]. Thus, BA and laser application can be said to positively affect fracture healing by regulating antioxidant enzyme activity and suppressing reactive oxygen species harmful effects.

The main limitation of the current study is its lack of micro computed tomographic analysis, which is accepted as a gold standard for evaluating fracture healing due to its robustness and reproducibility [41]. In micro computed tomography, many parameters—such as bone volume, the percentage of bone volume over tissue volume, trabecular thickness, trabecular separation, trabecular number, open pore volume, and the percentage of open porosity—are evaluated to assess bone mass and structure [8]. However, this technique is expensive and complicated for assessing healing ratios [42]. Previous studies have shown that the mRUST scoring system more highly correlates with micro-CT parameters; the distinction between "bridging" and "non-bridging" callus in the mRUST system, as well as the amount of callus in the fracture area, were also concluded to be better evaluated [43]. The lack of a critically sized (5 mm) defect on the femur is this study's other limitation [44]. Nevertheless, the fracture healing of small-diameter bone defects has been used for rats' femurs [45].

Conclusion

Thus, our results show that BA accelerates bone healing when used as a graft material with LLLT. Results suggest that a combination of BA and LLLT may improve bone formation, but further studies with different doses of BA are needed to better prove the benefits of association.

Acknowledgements The authors would like to thank Dr. Serkan YILDIRIM, Dr. Betul Apaydin YILDIRIM, Dr. Sitkican OKUR for their support in histopathological and biochemical analysis and statistical analysis, respectively.

Author contribution FT: literature search, study design, data collection and interpretation, manuscript preparation. LEY: statistical analysis, data collection and interpretation, manuscript preparation.

Data Availability The datasets generated during and/or analyzed during the current study are available from the corresponding author on reasonable request.

Declarations

Conflict of interest The authors declare no competing interests.

References

1. Foster AL, Moriarty TF, Zalavras C et al (2021) The influence of biomechanical stability on bone healing and fracture-related infection: the legacy of Stephan Perren. Injury 52:43–52. https://doi.org/10.1016/J.INJURY.2020.06.044
2. Wildemann B, Ignatius A, Leung F et al (2021) Non-union bone fractures. Nat Rev Dis Primers 7:1–21. https://doi.org/10.1038/s41572-021-00289-8
3. Govoni M, Vivarelli L, Mazzotta A et al (2021) Commercial bone grafts claimed as an alternative to autografts: current trends for clinical applications in orthopaedics. Materials 14:3290. https://doi.org/10.3390/MA14123290
4. Ulu M, Kütük N, Cıcık MF et al (2018) Effects of boric acid on bone formation after maxillary sinus floor augmentation in rabbits. Oral Maxillofac Surg 22:443–450. https://doi.org/10.1007/S10006-018-0729-3
5. Hakki SS, Bozkurt SB, Hakki EE, Nielsen FH (2021) Boron as boric acid ınduces mRNA expression of the differentiation factor tuftelin in pre-osteoblastic MC3T3-E1 cells. Biol Trace Elem Res 199:1534–1543. https://doi.org/10.1007/S12011-020-02257-X
6. Xu B, Dong F, Yang P, Wang Z, Yan M, Fang J, Zhang Y (2022) Boric acid inhibits RANKL-stimulated osteoclastogenesis in vitro and attenuates LPS-induced bone loss in vivo. Biol Trace Elem Res 1–10. https://doi.org/10.1007/S12011-022-03231-5. Online ahead of print.
7. Gizer M, Köse S, Karaosmanoglu B et al (2020) The effect of boron-containing nano-hydroxyapatite on bone cells. Biol Trace Elem Res 193:364–376. https://doi.org/10.1007/S12011-019-01710-W
8. Hadidi L, Ge S, Comeau-Gauthier M et al (2021) Local delivery of therapeutic boron for bone healing enhancement. J Orthop Trauma 35:165–170. https://doi.org/10.1097/BOT.0000000000001974
9. Cotler HB, Chow RT, Hamblin MR, Carroll J (2015) The use of low level laser therapy (LLLT) for musculoskeletal pain. MOJ Orthop Rheumatol 2:188–194. https://doi.org/10.15406/MOJOR.2015.02.00068
10. Theodoro LH, Rocha GS, Ribeiro VL et al (2018) Bone formed after maxillary sinus floor augmentation by bone autografting with hydroxyapatite and low-level laser therapy: a randomized controlled trial with histomorphometrical and immunohistochemical analyses. Implant Dent 27:547–554. https://doi.org/10.1097/ID.0000000000000801
11. Bayat M, Virdi A, Jalalifirouzkouhi R, Rezaei F (2018) Comparison of effects of LLLT and LIPUS on fracture healing in animal models and patients: a systematic review. Prog Biophys Mol Biol 132:3–22. https://doi.org/10.1016/j.pbiomolbio.2017.07.004
12. dos Santos DA, de Guzzi Plepis AM, da Conceição Amaro Martins V, et al (2020) Effects of the combination of low-level laser therapy and anionic polymer membranes on bone repair. Lasers Med Sci 35:813–821. https://doi.org/10.1007/S10103-019-02864-8
13. Sella VRG, do Bomfim FRC, Machado PCD et al (2015) Effect of low-level laser therapy on bone repair: a randomized controlled experimental study. Lasers Med Sci 30:1061–1068. https://doi.org/10.1007/S10103-015-1710-0
14. Deveci MZY, Gönenci R, Canpolat İ, Kanat Ö (2020) In vivo biocompatibility and fracture healing of hydroxyapatite-hexagonal boron nitridechitosan-collagen biocomposite coating in rats. Turkish J Vet Anim Sci 44:76–88. https://doi.org/10.3906/vet-1906-21

15. Özmeriç A, Tanoğlu O, Ocak M et al (2020) Intramedullary implants coated with cubic boron nitride enhance bone fracture healing in a rat model. J Trace Elem Med Biol 62:126599. https://doi.org/10.1016/J.JTEMB.2020.126599
16. Bosco AF, Faleiros PL, Carmona LR et al (2016) Effects of low-level laser therapy on bone healing of critical-size defects treated with bovine bone graft. J Photochem Photobiol, B 163:303–310. https://doi.org/10.1016/J.JPHOTOBIOL.2016.08.040
17. Fiset S, Godbout C, Crookshank MC et al (2018) Experimental validation of the radiographic union score for tibial fractures (RUST) using micro-computed tomography scanning and biomechanical testing in an in-vivo rat model. J Bone Joint Surg Am 100:1871–1878. https://doi.org/10.2106/JBJS.18.00035
18. Yoshioka T, Kawada K, Shimada T, Mori M (1979) Lipid peroxidation in maternal and cord blood and protective mechanism against activated-oxygen toxicity in the blood. Am J Obstet Gynecol 135:372–376. https://doi.org/10.1016/0002-9378(79)90708-7
19. Góth L (1991) A simple method for determination of serum catalase activity and revision of reference range. Clin Chim Acta 196:143–151. https://doi.org/10.1016/0009-8981(91)90067-M
20. Sun Y, Oberley LW, Li Y (1988) A simple method for clinical assay of superoxide dismutase. Clin Chem 34:497–500. https://doi.org/10.1093/CLINCHEM/34.3.497
21. Karayürek F, Kadiroğlu ET, Nergiz Y et al (2019) Combining platelet rich fibrin with different bone graft materials: an experimental study on the histopathological and immunohistochemical aspects of bone healing. J Craniomaxillofac Surg 47:815–825. https://doi.org/10.1016/J.JCMS.2019.01.023
22. Uysal T, Ustdal A, Sonmez MF, Ozturk F (2009) Stimulation of bone formation by dietary boron in an orthopedically expanded suture in rabbits. Angle Orthod 79:984–990. https://doi.org/10.2319/112708-604.1
23. Gölge UH, Kaymaz B, Arpaci R et al (2015) Effects of boric acid on fracture healing: an experimental study. Biol Trace Elem Res 167:264–271. https://doi.org/10.1007/S12011-015-0326-3
24. Ergul AB, Kara M, Karakukcu C et al (2018) High doses of boron have no protective effect against nephrolithiasis or oxidative stress in a rat model. Biol Trace Elem Res 186:218–225. https://doi.org/10.1007/S12011-018-1294-1
25. Hadrup N, Frederiksen M, Sharma AK (2021) Toxicity of boric acid, borax and other boron containing compounds: a review. Regul Toxicol Pharmacol 121:104873. https://doi.org/10.1016/J.YRTPH.2021.104873
26. Kennedy KC, Martinez SA, Martinez SE et al (2018) Effects of low-level laser therapy on bone healing and signs of pain in dogs following tibial plateau leveling osteotomy. Am J Vet Res 79:893–904. https://doi.org/10.2460/AJVR.79.8.893
27. Mostafavinia A, Farahani RM, Abbasian M et al (2015) Effect of pulsed wave low-level laser therapy on tibial complete osteotomy model of fracture healing with an intramedullary fixation. Iran Red Crescent Med J 17:12. https://doi.org/10.5812/IRCMJ.32076
28. Amid R, Kadkhodazadeh M, Sarshari MG et al (2022) Effects of two protocols of low-level laser therapy on the proliferation and differentiation of human dental pulp stem cells on sandblasted titanium discs: an ın vitro study. J Lasers Med Sci 13:1–6. https://doi.org/10.34172/JLMS.2022.01
29. Dalapria V, Marcos RL, Bussadori SK et al (2022) LED photobiomodulation therapy combined with biomaterial as a scaffold promotes better bone quality in the dental alveolus in an experimental extraction model. Lasers Med Sci 37:1583–1592. https://doi.org/10.1007/S10103-021-03407-W
30. Mota FCD, Belo MAA, Beletti ME et al (2013) Low-power laser therapy for repairing acute and chronic-phase bone lesions. Res Vet Sci 94:105–110. https://doi.org/10.1016/J.RVSC.2012.07.009
31. Renno AC, McDonnell PA, Parizotto NA, Laakso EL (2007) The effects of laser ırradiation on osteoblast and osteosarcoma cell proliferation and differentiation in vitro. Photomed Laser Surg 25:275–280. https://doi.org/10.1089/PHO.2007.2055
32. Coombe AR, Ho CTG, Darendeliler MA et al (2001) The effects of low level laser irradiation on osteoblastic cells. Clin Orthod Res 4:3–14. https://doi.org/10.1034/J.1600-0544.2001.040102.X
33. Saito S, Shimizu N (1997) Stimulatory effects of low-power laser irradiation on bone regeneration in midpalatal suture during expansion in the rat. Am J Orthod Dentofac Orthop 111:525–532. https://doi.org/10.1016/S0889-5406(97)70152-5
34. Schindl A, Schindl M, Pernerstorfer-Schon H, Schindl L (2000) Low-intensity laser therapy: a review. J Invest Med: the official publication of the American Federation for Clinical Research 48:312–326
35. Okur S, Okumus Z (2022) Effects of low-level laser therapy and therapeutic ultrasound on Freund's complete adjuvant-induced knee arthritis model in rats. Arch Rheumatol 37:i-xii. https://doi.org/10.46497/ArchRheumatol.2022.9409
36. Freddo AL, Rodrigo SM, Massotti FP et al (2009) Effect of low-level laser therapy after implantation of poly-L-lactic/polyglycolic acid in the femurs of rats. Lasers Med Sci 24:721–728. https://doi.org/10.1007/S10103-008-0627-2
37. Plumarom Y, Wilkinson BG, Willey MC et al (2021) Sensitivity and specificity of modified RUST score using clinical and radiographic findings as a gold standard. Bone Joint Open 2:796–805. https://doi.org/10.1302/2633-1462.210.BJO-2021-0071.R1
38. Zhu W, Murrell GAC, Lin J et al (2002) Localization of Nitric Oxide Synthases During Fracture Healing. J Bone Miner Res 17:1470–1477. https://doi.org/10.1359/JBMR.2002.17.8.1470
39. Duygulu F, Yakan B, Karaoglu S et al (2007) The effect of zymosan and the protective effect of various antioxidants on fracture healing in rats. Arch Orthop Trauma Surg 127:493–501. https://doi.org/10.1007/S00402-007-0395-7
40. Göktürk E, Turgut A, Baygu C et al (2009) Oxygen-free radicals impair fracture healing in rats. Acta Orthop Scand 66:473–475. https://doi.org/10.3109/17453679508995590
41. Bouxsein ML, Boyd SK, Christiansen BA et al (2010) Guidelines for assessment of bone microstructure in rodents using micro–computed tomography. J Bone Miner Res 25:1468–1486. https://doi.org/10.1002/JBMR.141
42. Wu Y, Adeeb S, Doschak MR (2015) Using micro-CT derived bone microarchitecture to analyze bone stiffness - a case study on osteoporosis rat bone. Front Endocrinol 6:80. https://doi.org/10.3389/FENDO.2015.00080
43. Cooke ME, Hussein AI, Lybrand KE et al (2018) Correlation between RUST assessments of fracture healing to structural and biomechanical properties. J Orthop Res 36:945–953. https://doi.org/10.1002/JOR.23710
44. Zwingenberger B, Vater C, Bell RL et al (2021) Treatment of critical-size femoral bone defects with chitosan scaffolds produced by a novel process from textile engineering. Biomedicines 9:1015. https://doi.org/10.3390/BIOMEDICINES9081015
45. Hakki SS, Dundar N, Kayis SA et al (2013) Boron enhances strength and alters mineral composition of bone in rabbits fed a high energy diet. J Trace Elem Med Biol 27:148–153. https://doi.org/10.1016/J.JTEMB.2012.07.001